



(RESEARCH ARTICLE)



Application of Integrated Geotechnical Investigation and 2D-Geoelectrical Tomography for Engineering Site (A Case Study of Ugbomro)

B. Osadipe*

Federal University of Petroleum Resources Effurun, Warri, PMB 1221 FUPRE road, Effurun, Warri 330102, Delta, Nigeria.

International Journal of Science and Research Archive, 2024, 13(02), 3250-3268

Publication history: Received on 12 November 2024; revised on 18 December 2024; accepted on 21 December 2024

Article DOI: <https://doi.org/10.30574/ijrsra.2024.13.2.2479>

Abstract

The current study was designed to find a permanent solution to engineering challenges involving building cracks and associated structural failures. An integrated 2-dimensional geo-electric tomography and geotechnical investigation were carried out in Ugbomro, Effurun, Delta state to aid in unravelling the causes of frequent building collapses in this fast-developing suburb, located in the Niger Delta region of Nigeria. Soil samples obtained for geotechnical investigation were tested and analysed to complement the resistivity survey using a combination of the Wenner and Dipole-Dipole arrays. This integrated approach resulted in more comprehensive data analysis and interpretations to strengthen contemporary knowledge in the study area. Wenner array provides good resolution of vertical and lateral changes in subsurface resistivity, supporting adequate delineation of horizontal structures such as sedimentary layers while the Dipole-Dipole array aids in mapping subtle subsurface features such as faults, joints and fractures and the associated geometry which could pose a threat to structural foundations and buildings within the study area. Geotechnical investigation involved drilling two boreholes to a depth of 15 metres each with samples taken at 0.8m vertical sample rate bringing the total samples collected to 32. For the electrical resistivity surveys, a spacing range of 5-30m was used with profile lengths of 100m in three different locations for both array types. Geotechnical investigation revealed predominant clayey sand composition from the surface to depths of 14m in BH 1 and 11m in BH 2 followed by predominant sand formations at the respective depths. Shallow foundational analysis carried out on both the chosen sites revealed allowable load-bearing capacities of 54 and 77kN/m² for footing of sizes 0.5-2.0m and founded at depths of 0.5-2.0m. For the electrical resistivity survey, the Wenner array results ranged from 6.5-1199 Ωm, 27-1199Ωm, and 52.9-1499 Ωm at locations A, B and C respectively with an average RMS error of 0.213 while the Dipole-Dipole array results ranged from 98-7560Ωm, 82-7980Ωm and 3-8503Ωm at locations A, B and C with an average RMS error of 0.39. The profile maps and resistivity profiles show similarities in the lithological structures delineated using the borehole logs and the resistivity surveys, which revealed clayey sand and sand are predominant formations within the general location.

Keywords: Soil sample; Subsurface Features; Load bearing; Shallow foundation

1. Introduction

Geo-electrical resistivity tomography is a geophysical method that is commonly used for subsurface imaging and characterisation. It is non-invasive and involves measuring the electrical resistivity of the ground to create 2D or 3D models of subsurface structures. This technique is widely applied in engineering and environmental studies, particularly in site characterisation and groundwater flow direction studies.

Given the fact that the near-surface geology of the Niger Delta is wholly soft and loose to semi-compacted strata, it is critical to complement all near geophysical surveys with geotechnical investigation, specifically for civil and engineering

* Corresponding author: B. Osadipe

projects. Geotechnical investigation is a bedrock for civil and engineering projects as it gives definite information about the subsoil types viz-a-viz the behaviors and characteristics.

This integrated geotechnical investigation and electrical resistivity surveys were carried out at the Ugbomro area of Delta State to determine the geotechnical and geo-electric characteristics and behaviour of the near-surface strata of the investigated site and to know the engineering properties of the subsoil types for engineering structural designs.

2. Review of Previous Works

Over the past few decades, Nigeria has experienced a significant increase in building collapses, leading to considerable loss of lives and properties (Adagunodo et al., 2015; Babalola, 2015). Site investigations are therefore critical to assess the properties of earth materials at specific locations and to evaluate their suitability for supporting structures (Youdeowei & Nwankwoala, 2013; Oghenero et al., 2014). Abam & Ngah (2014) assessed soil properties for pipeline installation along Nigeria's coastline using electrical resistivity surveys. They identified varying soil layers and shallow groundwater, indicating areas with high corrosivity potential, particularly in zones subject to frequent tidal flooding. Based on these findings, they recommended installing protective grounding systems for the pipeline.

ERT can be effective at delineating the interface between soil and bedrock, but resolution can be limited due to the scale of features or lack of contrast between soil and bedrock (Cheng, Q., Tao, M., Xi, C., & Binley, A. (2019)). In the Niger Delta region, Biola Osadipe et al. (2024) emphasized the need for geotechnical investigations before undertaking engineering projects. They observed high-compressibility clay and moderately compressible fine sand typical of swamp locations, recommending soil stabilization within the 0-3 meter depth range and concrete piling for load-bearing structures.

In another study, Osadipe et al. (2024) also suggested replacing peat and clay layers with stable soils, such as coarse sand, for swamp-based marginal field developments, with piling to stable strata for better load distribution. Nwankwoala et al (2014) worked on determination of Subsurface Geotechnical Properties for Foundation Design and Construction recommended that studies on the geotechnical characteristics of the area be carried out as it provides valuable data that can be used for foundation design and other forms of construction for civil engineering structures in order to minimize adverse effects and prevention of post construction problems.

Alaminiokuma & Chaanda (2020) used resistivity surveys to examine soil layers beneath cracked buildings at the Federal University of Petroleum Resources Effurun (FUPRE), finding a layer of low-resistivity clayey sand above a deeper sand layer. The presence of clay suggested uneven settling due to moisture variation, prompting recommendations for foundation reinforcement with pilings deeper than 2 meters. Airen & Emenim (2021) used the dipole-dipole array to map oil spill contamination in Delta State, identifying three main soil layers: sand, clayey sand, and clay. They noted that contamination appeared to affect the top two layers to a depth of approximately 20 meters.

Ibrahim Shuaibu and Rintong Babatunde (2022) carried out a geotechnical investigation of soils: a case study of a proposed residential development at no. 7, Sambo Close, Kaduna, Kaduna State, Nigeria. The sub-soil at the proposed site is underlain by deposits of reddish-brown fine Lateritic Soil to a depth of 2.00m depth explored. Juliet Emudianughe et al. (2022) conducted a geotechnical investigation in Ughelli Metropolis, identifying high-plasticity fat clay and low-plasticity lean clay. They found that subsurface soils with high water retention could lead to seasonal swelling and shrinking, causing stress on foundations. Avwenagha, E., Akpokodje, E., & Tse, A. (2014) worked on the Geotechnical Properties of Subsurface Soils in Warri, Western Niger Delta, Nigeria, the results revealed that three major subsoil types underlie the area characterised by dry, swampy and marshy ground conditions.

3. Theoretical Background

All resistivity methods employ an artificial source of current which is introduced into the ground through point or long line contacts. The procedure is to measure potentials at other electrodes in the neighbourhood of the current flow. Electrical methods are based on the material's resistivity or its inverse, which is conductivity. From the surface potential we have,

$$\Delta v = \frac{I\rho}{2\pi} \dots\dots\dots (1)$$

Where; I = current, ρ = resistivity, r = distance between electrodes.

Theoretically, a single-point current source can be achieved by placing a corresponding current source at infinity.

Determination of subsurface resistivities requires knowledge of the potential distribution in addition to the input current. Given two current electrodes A and B in Figure 3, when we apply equation 1, the potential at an arbitrary point M is

$$\Delta V = \frac{I\rho}{2\pi} \left[\frac{1}{c_1P_1} - \frac{1}{c_1P_2} \right] \dots\dots\dots(2)$$

Usually, the potential difference between two points is measured. In theory, the injecting (current) electrodes could be used to measure the potential difference. However, the influence of the resistances between the subsurface and current electrodes is not precisely known (Cheng et al., 1990). Thus, two potential electrodes are dedicated to detecting the response signal. If P1 and P2 are the potential electrodes (Figure 1, the potential difference between P1 and P2 becomes,

$$\Delta\Phi = \frac{I\rho}{2\pi} \left\{ \frac{1}{c_1P_1} - \frac{1}{c_1P_2} - \frac{1}{c_2P_1} + \frac{1}{c_2P_2} \right\} \dots\dots\dots(3)$$

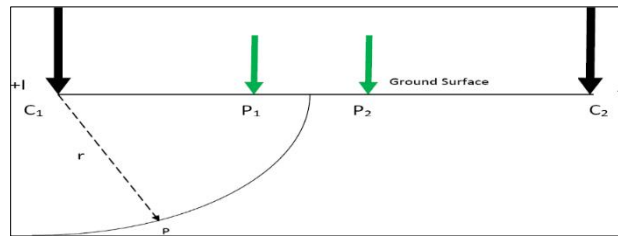


Figure 1 General four-electrode array configuration

This equation gives the potential that would be observed over a homogeneous half-space with a typical four-electrode configuration. The subsurface is typically heterogeneous so that the resistivity observed is apparent, that is, the resistivity of a homogeneous subsurface medium that would give the same resistivity value for the same electrode configuration. Apparent resistivity can be seen as a weighted average of the resistivities of the subsurface volume under the four electrodes. The apparent resistivity depends on the configuration of the electrodes and is determined by the injected current I and voltage. Thus, the apparent resistivity ρ_a is expressed as

$$\rho_a = G \frac{\Delta V}{I} \dots\dots\dots (4)$$

The geometric factor G in the above expression, which depends on the electrode configuration, is given as

$$G = 2\lambda / \left\{ \frac{1}{c_1P_1} - \frac{1}{c_1P_2} - \frac{1}{c_2P_1} + \frac{1}{c_2P_2} \right\} \dots\dots\dots (5)$$

• **Dipole-dipole array**

This array has been, and is still, widely used in resistivity and IP surveys because of the low EM coupling between the current and potential circuits. The arrangement of the

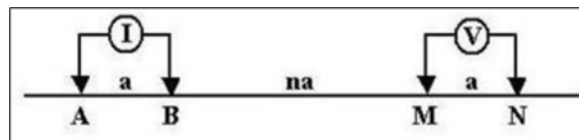


Figure 2 Conceptual diagram of a Dipole-dipole array and array formula

electrodes is shown in Figure 1.1. The spacing between the current electrodes pair, C2-C1, is given as “a” which is the same as the distance between the potential electrodes pair P1-P2. This array has another factor marked as “n” in Figure 1.1. This is the ratio of the distance between the C1 and P1 electrodes to the C2-C1 (or P1-P2) dipole length “a”. For surveys with this array, the “a” spacing is initially kept fixed at the smallest unit electrode spacing and the “n” factor is increased from 1 to 2 to 3 until up to about 6 to increase the depth of investigation.

$$\rho_A = \frac{V}{I} \pi a n (n + 1)(n + 2) \dots\dots\dots(6)$$

- **Wenner array**

This is a frequent array that was popularized by the pioneering work carried out by The University of Birmingham research group (Griffiths and Turnbull 1985; Griffiths, Turnbull, and Olayinka 1990). Many of the early 2-D surveys were carried out with this array. The "normal" Wenner array is technically the Wenner Alpha array. For a four-electrode array, there are three possible permutations of the positions of the electrodes (Carpenter and Habberjam 1956). Wenner Alpha array has a moderate depth of investigation. The signal strength is inversely proportional to the geometric factor used to calculate the apparent resistivity value for the array. The geometric factor for the Wenner array is $2\pi a$. This is smaller than the geometric factor for other arrays. Among the common arrays, the Wenner array has the strongest signal strength. This can be an important factor if the survey is carried out in areas with high background noise. One disadvantage of this array for 2-D surveys is the relatively poor horizontal coverage as the electrode spacing is increased (Figure 1.2). This could be a problem if one surveys a relatively small number of electrodes.

$$\rho_A = 2\pi a \frac{V}{I} \text{ -----(7)}$$

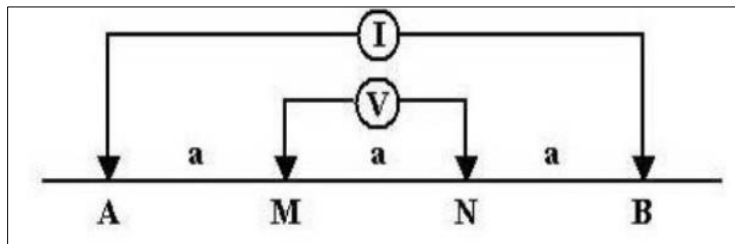


Figure 3 conceptual diagram of a Wenner array and array formula

3.1. Location and Geology of Study Area

The general topography of the study area is a relatively flat plain, and it is surrounded by residential buildings and main roads. This study area receives approximately 2770 mm of rainfall per year. The average temperature is between 28 °C (minimum) and 32 °C (maximum) with average relative humidity varying from 64 % to 94 %. The dry season lies between November to April and the wet season lies between May and December.

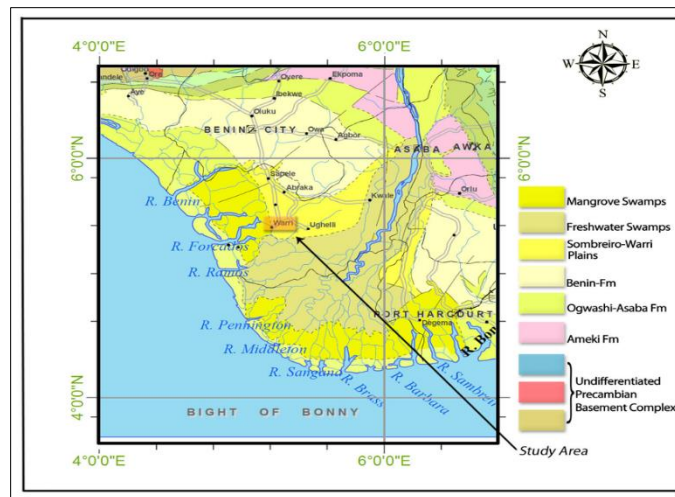


Figure 4 Geological map of the western Niger Delta showing the location of the Effurun-Warri Metropolis (Adapted from NGS, 2004)

3.2. Geological features of the study area

Ugbomro is located within the Niger Delta which is located in the Gulf of Guinea at a formal triple junction of the South Atlantic rifting between latitude 4°N to 7°N and longitude 5°E to 8°E covering an area of about 108,900km² (Whiteman, 1982). It extends from the Calabar flank and the Abakaliki Trough in eastern Nigeria to the Benin flank in the west and it opens to the Atlantic Ocean in the south. The development of the Niger Delta resulted from the formation of the Benue trough as a failed arm of a triple junction associated with the separation of African and South American Plates and the

subsequent opening of the South Atlantic (Whiteman, 1982). The Benue-Abakaliki trough was filled with sediments during the early Cretaceous time which later underwent folding, faulting, and uplift with subsidence of the adjacent Anambra basin to the west and Afikpo syncline to the east during the Santonian. The sedimentary fill of the Niger Delta basin is subdivided into three (3) broad lithofacies units, which include the marine shale (Akata Formation); marginal marine sandstones, shales and clays (Agbada Formation); and massive continental sandstones (Benin Formation) (Weber and Daukoru, 1975). It is underlain by Quaternary Warri deltaic sand (Etu-Efeotor and Akpokodje, 1990). The sediments overly the Coastal Plain sand comprising silt, sand and clay. The sands are loose, porous, poorly sorted and lateritic. Small amounts of gravel and thin clay horizons are sometimes present at greater depths (Avbovbo, 1978).

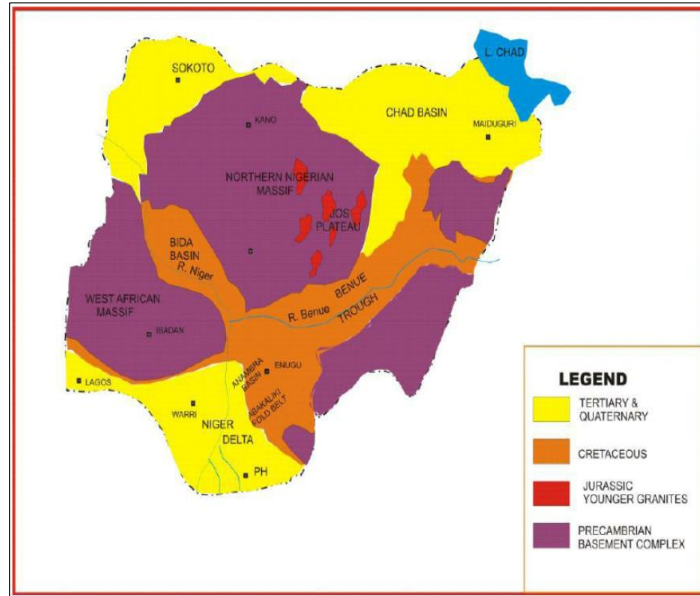


Figure 5 Map of Delta State showing the geology of the study area.

4. Materials and Methods

4.1. Electrical Equipment

Equipment and materials that were used during the electrical resistivity surveys are listed below

- **Measuring Tape:** A measuring tape was essential for ensuring accurate and consistent electrode spacing throughout the survey, regardless of the specific array configuration employed.



Figure 6 A Reel of Measuring Tape

- **Ohmega Terameter:** this was used to measure and introduce current into the subsurface through the electrode at a particular frequency and number of cycles. It was also used to measure the apparent resistance to the flow of current.



Figure 7 Ohmega Terameter



Figure 8 Cable reels

- **Reels of Cable:** This was used to connect the electrodes to the terameter to allow the flow of current into the subsurface during the survey.
- **Electrodes:** these were fixed to the ground, and the current was introduced into the subsurface through them from the terameter.

4.2. Methodology for Wenner Array

The field data acquisition was carried out after a reconnaissance visit to the study area. The coordinate values of the profile were collected using Germaine Geographical Positioning System (GPS). Hammering of electrodes numbering 0,1,2 and 3 were fixed into the ground at selected intervals of 5m along the profile line for the array. The unit electrode spacing was 5m to ensure high resolution from the subsurface geoelectrical image. The profile length was 100.00m. The maximum electrode spacing was 15.00m, giving the maximum depth of investigation at about 37m. 2-D ERT survey data were acquired using the Ohmega Terameter Resistivity meter while employing the Wenner electrode array.

For the first measurement, $n=1$, $a = 5$, $K = 3.142$ which stands for serial number 1. The four electrodes are positioned at (0m, 5m, 10m, and 15m), which corresponds to the (C1, P1, P2, C2) positions for the current (C1 and C2) and potential electrodes (P1 and P2) on the particular profile. The next serial number 2 is a forward shift of electrode positions by 5m each. The electrodes assume the new positions (5m, 10m, 15m, and 20m). The next serial number 3 is a forward shift of electrode positions by 5m each (10,15,20 and 25m). However, the C1 and C2 difference of 15m is maintained throughout the measurements while the P1 and P2 difference of 5m is maintained throughout the measurements. 100m profile length is observed for seventy-two ($4 * 18$) electrodes. In each case, the circuitry is completed by connecting the electrodes to the Ohmega Terameter Resistivity meter via single-core cables. The resistance of the formation was measured which was then transformed to apparent resistivity through the transformation equation.

$$\rho_a = KR, \dots\dots\dots (8)$$

Where ρ_a is apparent resistivity, R is resistance, and K is the Geometrical factor.

4.3. Methodology for Dipole-Dipole

The field data was acquired perpendicular to the Wenner traverse line to achieve a 2D ERT. The coordinate values of the profile were also collected using Germaine Geographical

Positioning System (GPS). Hammering of electrodes numbering 0,1,2 and 3 were fixed into the ground at selected intervals of 5m along the profile line for the array. The unit electrode spacing was 5m to ensure high horizontal resolution from the subsurface geoelectrical image. The profile length was 100m. The maximum electrode spacing was 15.00m, giving the maximum depth of investigation at about 25m. 2-D ERT survey data were acquired using the Ohmega Terameter Resistivity meter while employing the Dipole-dipole electrode array.

For the first measurement, $n=1$, $a = 5$, $K = 94.26$ which stands for serial numbers 1 to 18. The four electrodes are positioned at (0m, 5m, 10m, and 15m), which corresponds to the positions for the current (C1 and C2) and potential electrodes (P1 and P2) on the particular profile. The next serial number 2 is a forward shift of potential electrode positions by 5m each. The electrodes assume the new positions (0m, 5m, 15m, and 20m). The next serial number 3 is a forward shift of potential electrode positions by 5m each (0m, 5m, 20m, and 25m) until the last serial number of electrode positions (0m, 5m, 95m, and 100m). However, the C1 and C2 difference of 5m is maintained throughout the measurements while the P1 and P2 of 5m incremental is also maintained throughout the measurements for the three traverses of ($n=1$).

For the second reading, the above scenario applied to all the traverses with $n=2$ to 5, and $a=5$ with varying geometrical factors respectively. The resistance of the formation was measured, which was then transformed to apparent resistivity through the transformation equation.

4.4. Geotechnical Materials and Methodology

Below is the list of materials employed to carry out the geotechnical investigation

- Manual drilling machine
- Differential Global Positioning System
- Sample bag
- Plastic Cooler
- Field Sheet

4.4.1. Setting Out Borehole Point

The Differential Global Positioning System (DGPS) was used to translocate from a known origin to determine the locations of the borehole test points. Before the start of the boring of holes in selected locations on the site, the locations were marked with a borehole number (ID) so that the drillers could identify them. BH1 and BH2 have coordinates of N50 34' 26.29", E50 50' 01.13" and N50 34' 29.13", E50 50' 01.38"

4.4.2. Boring Activity

The manual drilling method engages the manual auger. This method of boring engages the effort of the driller and the rotation of the drilling auger. At the location, the auger is screwed tight to one end of the drilling stem and positioned on the point. While in the position, the driller pushes hard on the crossbar as he turns it clockwise with gloved hands. The rotation of the auger under the effort of the driller cuts the soil which is held in the cup-shaped auger. Once the cup is full, it is retrieved to the ground surface and emptied. After emptying, it is again returned to the hole, and the process is repeated until the target depth is attained.



Figure 9 A boring activity with a manual drilling rig

4.4.3. Soil Sampling

Boreholes were sampled to obtain samples for laboratory analysis. Disturbed samples were collected from the borehole using the drilling spoils. To ensure sample integrity, samples were properly labelled and placed in watertight bags, while undisturbed samples were collected using an open-tube sampler. The tube's ends were properly sealed, labelled, and secured. The samples were adequately protected and preserved during the investigation before being transported to the laboratory for analysis. Between the ground surface and a depth of 1.5m, groundwater was discovered. As a result, groundwater may pose challenges to the excavation of any type of shallow foundations on the site. Water samples from the two boreholes were collected for chemical testing in the laboratory.

5. Results for Geotechnical Investigation

5.1. Soil Stratigraphy

The boreholes explored revealed a formation of clayey sand overlying a formation of sand. Borehole BH1 revealed a formation of clayey sand to 14.0m below the existing ground level while the sand is between 14m to 15m below the existing ground level. In borehole BH2, the clayey sand is observed to a depth of 11.0m below the existing ground surface while the sand is between 11m to 15m below the existing ground level. The maximum depth of investigation is 15m

Table 1 Strata of BH-01

Strata	Description	Average depth range (m)
1	CLAYEY SAND, brown	0 - 14
2	SAND	14.0 - 15.0

Table 2 Strata of BH-02

Stratum No.	Description	Average depth range (m)
1	CLAYEY SAND, brown	0 - 11.0
2	SAND	11.0 - 15.0

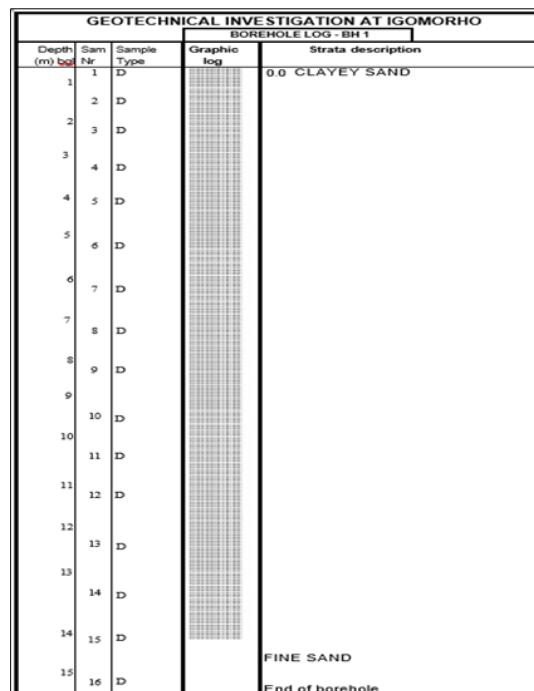


Figure 10 BH-01 Log

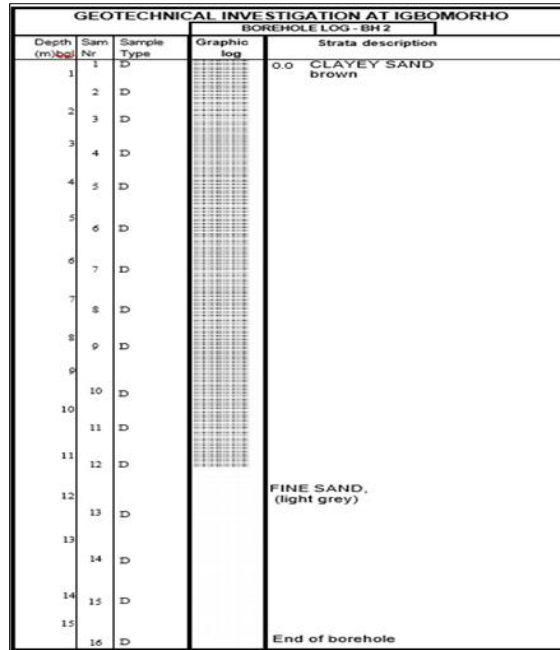


Figure 11 BH-01 Log

5.1.1. CLAYEY SAND

The encountered formation of clayey sand is characterized by moderate compressibility and moderate moisture content. The deposit is homogeneous in its composition, though non-uniform in thickness. However, it is competent in its present state to carry building structure as long as the allowable bearing capacity as stated in this report is not exceeded. The parameters of the clayey sand formation are presented in the table below.

Table 3 Profile of the Clayey Sand Stratum.

S/N	Parameter	Design values
1	Moisture content (%)	36
2	Bulk unit weight (kN/m ³)	17.32
3	Dry unit weight (kN/m ³)	12.82
4	Submerged unit weight (kN/m ³)	7.51
5	Liquid limit (%)	55
6	Plastic limit (%)	28
7	Plasticity index (%)	27
8	Shear strength (kN/m ²)	47

5.1.2. FINE SAND

The stratigraphy of silty fine sand encountered is characterized by low compressibility and low moisture content. Presented below are the design values for the sand.

Table 4 Profile of the FINE SAND Stratum.

S/N	Parameter	Design Values
1	Moisture content (%)	30
2	Bulk unit weight (kN/m ³)	18.36
3	Dry unit weight (kN/m ³)	14.10

5.2. Bearing Capacity Analysis – Shallow Foundation

5.2.1. Design of Square Pad Footing

The ultimate bearing capacity, Q_u , for shallow square pad foundations of buildings on cohesive soils, using Terzaghi’s equation as:

$$Q_u = 7.4c + \gamma \cdot D_f \cdot N_q \dots\dots\dots(9)$$

where

- γ = Unit weight of soil at depth
- D_f = Depth of foundation
- c = Soil cohesion
- N_q = Bearing capacity factor

Foundation with square footing of width, B , = 0.50, 1.0, 1.50 and 2.0m founded at depths, D_f , between 0.50 and 2.0m are considered in this report.

The table below presents a summary of both the ultimate and allowable bearing capacities for foundations with square footing of different sizes placed at different depths.

Table 5 Bearing Capacity Values, kN/m^2 for Foundation with Square Footing

Foundation Depth (m)	Bearing Capacity (kN/m^2)	
	Ultimate	Allowable
0.5	136	54
1.0	149	60
1.5	166	67
2.0	192	77

The above results are presented in chart formats in the charts below. These charts are for both the ultimate and allowable bearing capacities for foundations with square footings of 0.50, 1.0, 1.50 and 2.0m wide placed at depths between 0.50m and 2.0m below the existing ground surface

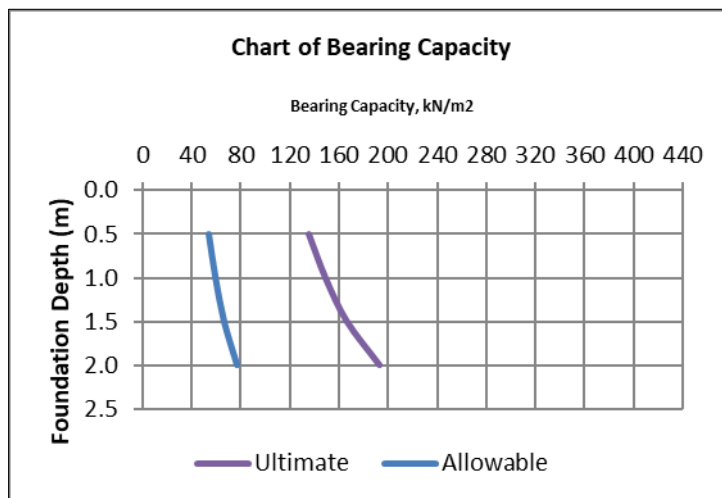


Figure 12 Bearing Capacity Chart at different Depths of Footing

5.2.2. Settlement Analysis

The settlement from the anticipated imposed load on this site shall be obtained from the sum of both the immediate settlement and the consolidation settlement according to Karl Terzaghi.

5.2.3. Immediate Settlement

The clayey sand encountered at the upper layer in this investigation when loaded with the imposed load, shall undergo deformation with volume change. The vertical deformation due to the change in shape is the

immediate settlement, ρ_i .

This immediate settlement, ρ_i , of the building structure according to Terzaghi is given by

$$\rho_i = q * B * (1 - \nu^2) * I / E \dots\dots\dots (10)$$

where

q = uniform intensity of pressure, kPa

B = width of the pad footing, m

I = Influence factor = 0.82

ν = Poisson's ratio of soil (= 0.4) for drained condition

E_u = undrained modulus of deformation of the soil beneath the foundation

From the above formula, the immediate settlement of the foundation footing on the site is as in the below table. Values from allowable bearing capacity have been used in the settlement calculations.

Table 6 Summary Table for Immediate Settlement, mm

Foundation depth (m)	Settlement, ρ_i , (mm)			
	B = 0.5m	B = 1.0m	B = 1.5m	B = 2.0m
0.5	2	3	5	7
1.0	2	3	5	6
1.5	2	3	5	6
2.0	2	3	5	6

Table 7 Summary table for Consolidation Settlement, mm

Foundation depth (m)	Settlement, ρ_c , (mm)			
	B = 0.5m	B = 1.0m	B = 1.5m	B = 2.0m
0.5	190	281	342	388
1.0	191	283	345	382
1.5	194	289	353	402
2.0	201	302	372	424

The consolidation settlement, ρ_c , is obtained from the formula

$$\rho_{con} = H * [C_c / (1 + e_o)] * \log_{10} [(P_o + \Delta P) / P_o] \dots\dots\dots (11)$$

Where

H = thickness of consolidating layer, = 1.5B (m)

C_c = compression index of the clay = 0.009(LL-10)

e_o = initial void ratio of the clay layer

P_o = overburden pressure on the consolidating layer, kPa

ΔP = imposed pressure from an applied load, kPa

From the above formula, the consolidation settlement of the foundation footing on the site is as in the below table

Table 8 Summary Table for Consolidation Settlement, mm

Foundation depth (m)	Consolidation Settlement, ρ_c , (mm)			
	B = 0.5m	B = 1.0m	B = 1.5m	B = 2.0m
0.5	192	284	347	395
1.0	193	286	350	388
1.5	196	292	358	408
2.0	203	305	377	430

5.2.4. Total Settlement ρ_t Calculation

The total settlement is the sum of the immediate and consolidation settlements.

$$\rho_t = \rho_i + \rho_c \dots\dots\dots(12)$$

as in the table below

Table 9 Summary Table for Total Settlement, mm

Foundation depth (m)	Settlement, ρ_t , (mm)			
	B = 0.5m	B = 1.0m	B = 1.5m	B = 2.0m
0.5	192	284	347	395
1.0	193	286	350	388
1.5	196	292	358	408
2.0	203	305	377	430

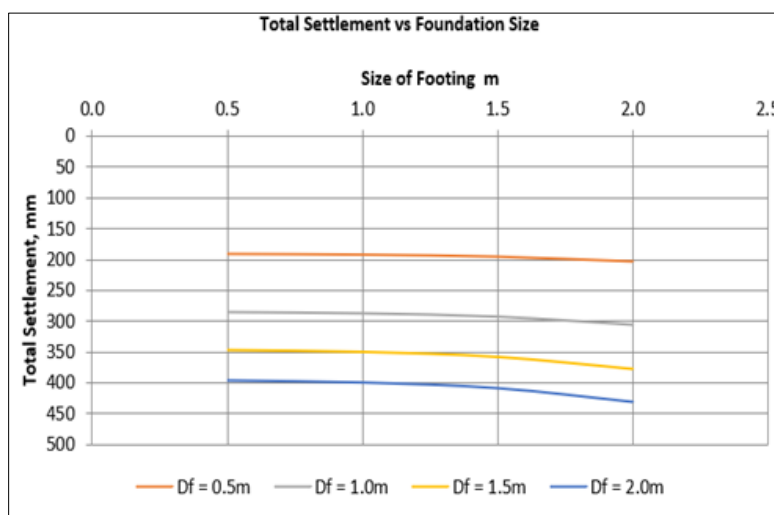


Figure 13 Footing Size versus Total Settlement Chart for Allowable Capacities

The above total settlement values are presented in chart formats in the chart below.

5.3. Results for Electrical Surveys

5.3.1. Location A

Wenner Model

- The resistivity values between 6.51 and 1199 Ω m are observed in the investigation with an RMS error of 0.22.
- Two major subsoil types are identified. These are, Clayey Sand and Sand
- The resistivity values ranging between 6.51 and 14.0 Ω m are attributed to unconsolidated wet topsoil.
- The wet topsoil is observed literally from 50 to 90m between depths of 0 to 0.7m
- The Clayey Sand is widely distributed along the transverse with resistivity values ranging between 20.5 to 97 Ω m
- The shallow near-surface Clayey Sand is observed literally from 33 to 90m with a depth range of 0 to 4m
- The deep near-surface Clayey Sand is observed literally from 15 to 33m with a depth range of 5 to 25m.
- The sand has resistivity values between 310 to 1199 Ω m

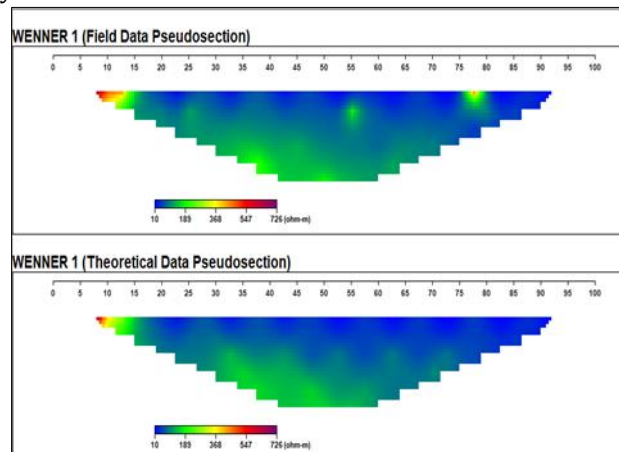


Figure 14 Theoretical and field data Pseudosection (Wenner traverse 1)

The Sand is observed along the transverse from 7 to 12m and from 30 to 90m with a depth range of 5 to 25m.

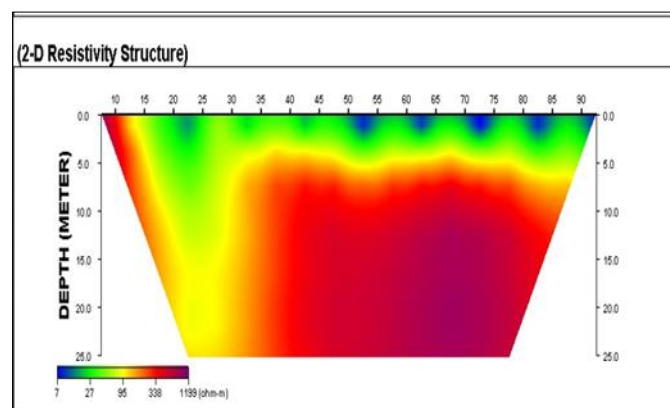


Figure 15 2D resistivity structure (Wenner traverse 1)

Dipole-Dipole Model

- The resistivity values between 98 and 7560 Ω m are observed with an RMS error of 0.35
- The 2D Resistivity structure shows that there is no fault within the depth of investigation. There is continuity of the subsoil types from a lateral distance of 0 to 90m
- Two major subsoil types are identified. These are Clayey Sand (CS) and Sand/Consolidated Sand.
- The wet topsoil exhibits resistivity values ranging between 98 and 120 Ω m with lateral distance from 0 to 90m between 0 to 2m depth.

- The Clayey Sand is laterally distributed along the transverse with resistivity values ranging between 267 to 512Ωm
- The Clayey Sand is observed literally from 10m to 90m with a 2 to 6m depth range.
- The sand is observed with resistivity values between 1510 to 6012Ωm with lateral distance from 10m to 90m and depth from 7 to 12m depth

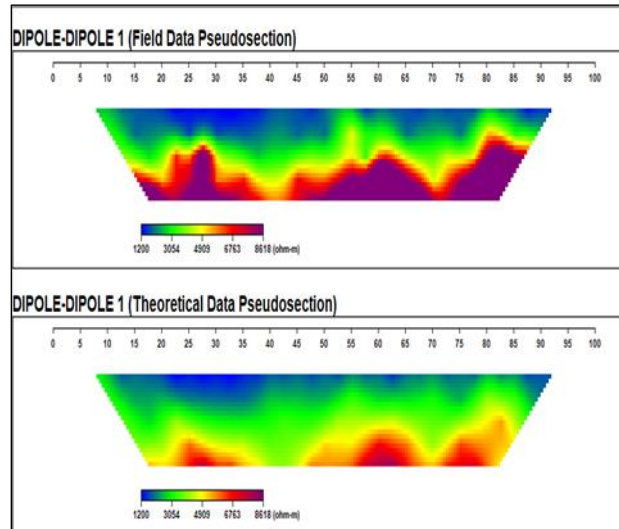


Figure 16 Theoretical and field data Pseudosection (Dipole-dipole traverse 1)

Consolidated sand is suspected below the sand level based on the high resistivity values

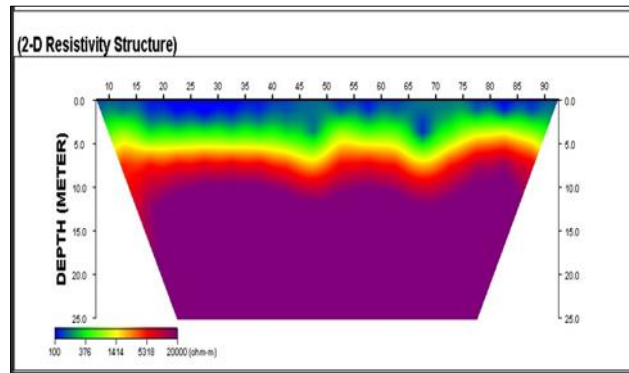


Figure 17 2D resistivity structure (Dipole-dipole traverse 1)

5.3.2. Location B

Wenner Model

- The resistivity values between 27 and 1199Ωm are observed in the investigated area with an RMS error of 0.17.
- Two major subsoil types are identified. These are, Clayey Sand and Sand
- The Clayey Sand is widely distributed along the transverse with resistivity values ranging between 27 to 192Ωm
- The shallow near-surface Clayey Sand is observed to be saturated with water with a depth thickness of 6 to 10m with lateral distance from 10 to 22m
- The Clayey Sand is observed literally from 10 to 37m, 52 to 61m and 72 to 88m with a depth range from 5 to 22m.
- The sand has resistivity values between 340 to 1196Ωm
- The shallow near-surface Sand is observed literally from 0 to 72m with a depth range of 0 to 4m
- The deep near-surface Sand is also observed at a depth of 12 to 25m with a lateral distance of 25 to 65m

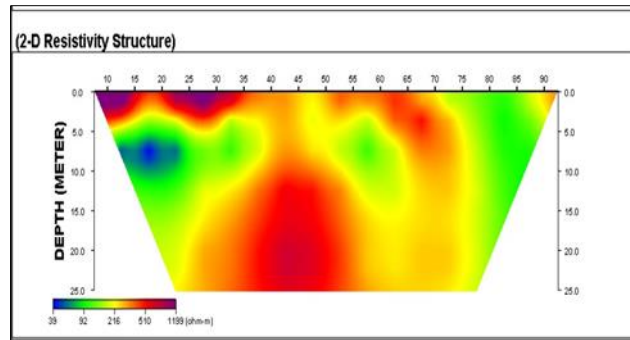


Figure 18 Theoretical and field data Pseudosection (Wenner traverse 2)

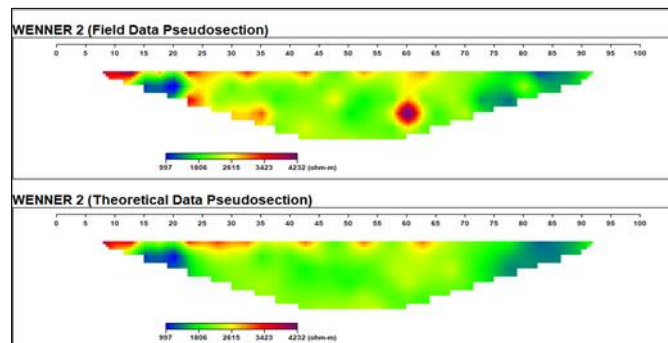


Figure 19 2D resistivity structure (Wenner traverse 2)

Dipole-Dipole Model

- The resistivity values between 82 and 7980Ωm are observed with an RMS error of 0.35.
- The 2D Resistivity structure shows that there is no fault within the depth of investigation. There is continuity of the subsoil types from a lateral distance of 0 to 90m
- Two major subsoil types are identified. These are Clayey Sand (CS) and Sand/Consolidated Sand.
- The wet topsoil is observed to exhibit resistivity values ranging between 97 and 150Ωm with lateral distance from 0 to 90m between 0 to 1.5m depth
- The Clayey Sand is laterally distributed along the traverse with resistivity values ranging between 362 to 1398Ωm
- The Clayey Sand is observed literally from 10m to 90m with a depth range of 3.5 to 7m.
- The sand is observed with resistivity values between 2680 to 6240Ωm with a lateral distance from 10m to 90m and depth from 7 to 25m depth

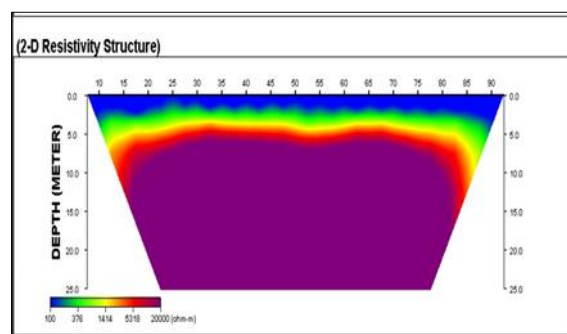


Figure 20 Theoretical and field data Pseudosection (Dipole dipole traverse2)

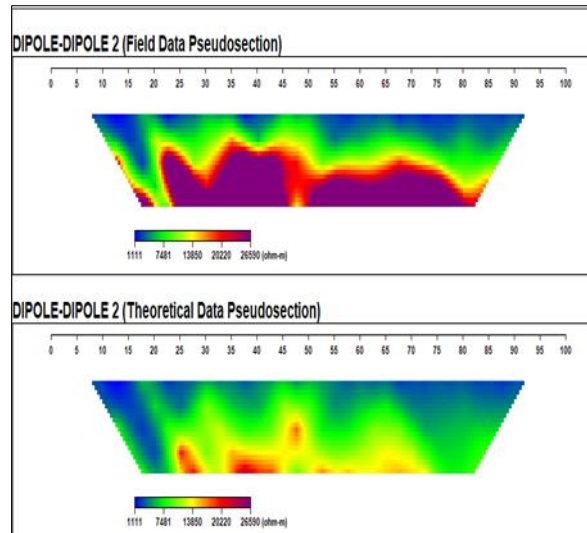


Figure 21 2D resistivity structure (dipole-dipole traverse 2)

5.3.3. Location C

Wenner Model

- The resistivity values between 52.9 and 1497 Ω m are observed in the investigated area with an RMS error of 0.25.
- Two subsoil types are identified. These are Clayey Sand and Sand
- The Clayey Sand is widely distributed along the traverse with resistivity values ranging between 48 to 260 Ω m
- Clayey Sand is observed towards the right-hand side of the structure suspected to be saturated with water with a lateral distance from 57 to 78m between 2 to 25m depth
- The shallow near-surface Clayey Sand is observed literally from 4 to 11m with a depth range of 22 to 37m and 45 to 52m to the East.
- The sand is observed to have resistivity values between 502 and 1499 Ω m
- The shallow near-surface sand is observed literally from 0 to 75 with a depth range of 0 to 2m
- The deep near-surface sand is observed at a depth of 15 to 55m with a lateral distance of 15 to 25m

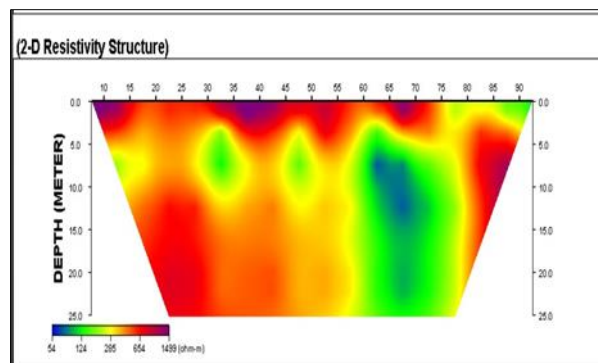


Figure 22 Theoretical and field data Pseudosection (Wenner traverse 3)

Dipole-Dipole Model

- The resistivity values between 29 and 8503 Ω m are observed with an RMS error of 0.47.
- The 2D Resistivity structure shows that there is no fault within the depth of investigation. There is continuity of the subsoil types from a lateral distance of 0 to 90m
- Two major subsoil types are identified. These are Clayey Sand (CS) and Sand/Consolidated Sand.

- The Clayey Sand is laterally distributed along the transverse with resistivity values ranging between 34 to 286Ωm
- The Clayey Sand is observed literally from 10 to 90m with a depth range of 3.5 to 5m.
- The sand is observed with resistivity values between 348 to 8503Ωm with a lateral distance from 0 to 90m and a depth from 6 to 11m
- Consolidated Sand is suspected below the sand level based on the high resistivity values

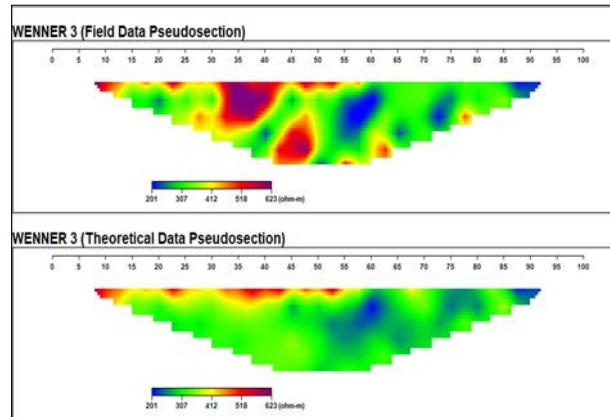


Figure 23 2D resistivity structure (Wenner traverse 3)

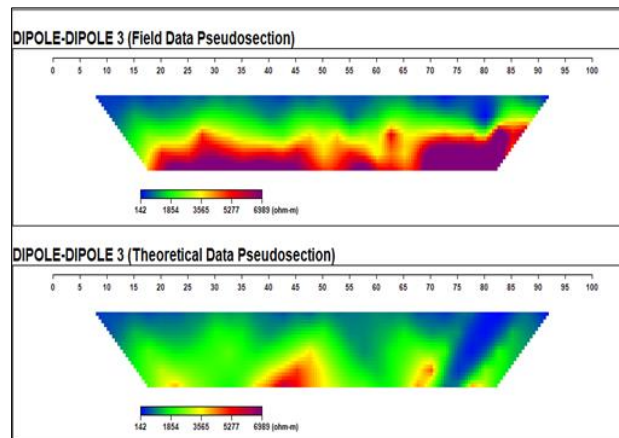


Figure 24 Theoretical and field data Pseudosection (Dipole-dipole traverse 3)

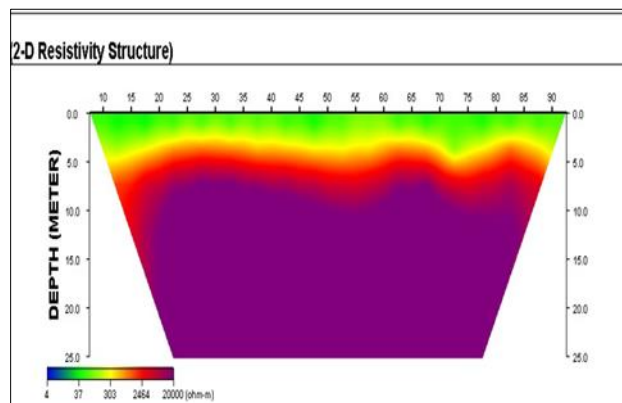


Figure 25 2D resistivity structure (dipole-dipole traverse 3)

6. Conclusion

The integrated geotechnical investigation and 2D geo-electrical tomography were carried out to understand the distribution, dipping, characteristics and behaviours of subsoil types for an engineering site at Ugbomro and its environs. This survey is to proffer remedy for any subsurface anomaly that may contribute to structural failure in the investigated area.

From the field geophysical investigation, Clayey sand is widely distributed in the investigated area with resistivity values ranging between 20.5 and 260 Ω m. The sand body is observed to be deep near-surface with resistivity values ranging between 310 and 1499 Ω m

The dipole-dipole geoelectric array was employed in this survey to delineate near-surface faults within the area of investigation. The Dipole-dipole array revealed a continuity of the two major subsoil types viz-a-viz the clayey sand and sand.

From the geotechnical field investigations, clayey sand was observed from the ground surface at a depth of 14.0m in borehole BH1 and 11.0m in borehole BH2. Underlying the clayey sand formation is a stratum of fine sand observed from the depth of 14m and 11m to the final 15.0m depth for BH1 and BH2 respectively.

The average undrained shear strength value of the clayey sand is about 39kN/m² and of low plasticity with plasticity indices between 22 and 31%

From the analysis of the samples obtained from the boreholes, it is observed that the site possesses allowable bearing capacity values between 54 and 77kN/m² with accompanying total settlement values between 192 and 430mm for footings with sizes, B (m), between 0.5m and 2.0m founded at depths between 0.5 and 2.0m.

Recommendations

It is recommended that for buildings, its footings shall be founded at a minimum depth of 1.0m below the existing ground level to forestall the seasonal variations associated with footings founded at a shallow depth.

Shallow foundation only is considered in this report because it is not anticipated that deep pile foundation shall be employed to support the buildings.

Limitations

This investigation was carried out by accepted geophysical and geotechnical engineering practices. The conclusion and recommendations reached in the report are based on the data obtained from geo-electrical resistivity arrays and geotechnical investigation (soil boring and laboratory analysis). It is not anticipated that the soil conditions will vary significantly from those described. However, slight variations resulting from the heterogeneous nature of soils should be anticipated.

Compliance with ethical standards

Acknowledgements

I acknowledge the Editor-in-chief and the Reviewers for their selfless services in improving this research work.

References

- [1] Abam, T. K. S., & Ngah, S. A. (2014). Geo-electric characterization of the beach ridge in Escravos, Western Niger Delta, Nigeria. *Journal of Emerging Trends in Engineering and Applied Sciences*, 5(3), 211 - 216.
- [2] Akpoborie, I. A., Ekakitie, O. A. and Adaikpoh, E. O. (2000). The Quality of Groundwater from Dug wells in parts of the Western Niger Delta. *Knowledge*. Revised. 2(5), pp. 72-79.
- [3] Adagunodo et al., 2015 Geophysical investigation into the integrity of a reclaimed open dumpsite for civil engineering purposes. *Interciencia Journal* ISSN:0378-1844

- [4] Alaminiokuma, G., & Chaanda, M. (2020). Geophysical Investigation of Structural Failures Using Electrical Resistivity Tomography: A Case Study of Buildings in FUPRE, Nigeria. *Journal of Earth Sciences and Geotechnical Engineering*, 15-33.
- [5] Airen, O. J., & Emenim, V. (2021). The use of Geoelectrical Method to Investigate the Extent of Hydrocarbon Contamination in Okpare-Olomu Community, Delta State, South-South Nigeria. *London Journal of Research in Science: Natural and Formal*, 21(4), 49 - 56.
- [6] Avwenagha, E., Akpokodje, E., & Tse, A. (2014). Geotechnical Properties of Subsurface Soils in Warri, Western Niger Delta, Nigeria. *Journal of Earth Sciences and Geotechnical Engineering*, 89-102.
- [7] Avbovbo, A.A. (1978) Tertiary Lithostratigraphy of Niger Delta. *American Association of Petroleum Geologists Bulletin*, 62, 295-300.
- [8] B. Osadipe, I. Adesokan, B. Olusola, A. Shittu, and A. Ifediora (2024), Examination of Geotechnical Properties of Structures of a Swamp Marginal Field Development in the Niger Delta, <https://doi.org/10.2118/221688-MS>
- [9] B. Osadipe I. Adesokan, B. Olusola, A. Shittu and A. Ifediora (2024), Geotechnical Site investigation for a proposed Marginal Field Development in a Swamp location, <https://doi.org/10.2118/221667-MS>
- [10] Cheng, Q., Tao, M., Xi, C., & Binley, A. (2019). Evaluation of electrical resistivity tomography (ERT) for mapping the soil–rock interface in karstic environments. *Environmental Earth Sciences*, 1-43.
- [11] Cheng et al; (1990). 2D and 3D resistivity imaging: Theory and field design. *Scientific Research and Essays Vol. 5(23)*, pp. 3592-3605
- [12] Etu-Efeotor, J.O. and Akpokodje, E.G. (1990) Aquifer Systems of the Niger Delta. *Journal of Mining and Geology*, 26, 279-285.
- [13] Ibrahim Shuaibu, Rintong Babatunde (2022), Geotechnical Investigation of Soils: A Case Study of a Proposed Residential Development At No. 7, Sambo Close, Kaduna, Kaduna State, Nigeria Vol. 24 No. 4 March 2022.
- [14] Juliet Emudianughe (2022), Geotechnical Investigation of Proposed Site for Building Suitability Using Geological and Geophysical Methods in Ughelli Metropolis, Vol 6, No 2(2022)
- [15] Nwankwoala, H., Amadi, A., Ushie, F., Warmate, T., & Eze, C. (2014). Determination of Subsurface Geotechnical Properties for Foundation Design and Construction in Akenfa Community, Bayelsa State, Nigeria. *Journal of Earth Sciences and Geotechnical Engineering*, 130-135.
- [16] Weber and Daukoru, 1975. *Jour. Min. Geol.*, 12, 9-12.
- [17] Whiteman, A.J. (1982) Nigeria, Its Petroleum Geology, Resources and Potential. *Petroleum Geology of the Niger Delta*. Graham and Trotman Publishing, London, 1 and 2, 251-269, 104-110.
- [18] Youdeowei, P., & Nwankwoala, H. (2013). Suitability of soils as bearing media at a freshwater swamp terrain in the Niger Delta. *Journal of Geology and Mining Research*, 58-64.